$\mathcal{H}_\infty$ Control of Unstable, Uncertain Systems Using Horowitz Bounds

Carl-Magnus Fransson*, Bengt Lennartson*, Claes Breitholtz*,
Anders Bondeson**, Yueqiang Liu**

* Department of Signals and Systems, Control and Automation Laboratory
** Department of Electromagnetics, EURATOM-NFR/Fusion Association
Chalmers University of Technology, SE-412 96 Göteborg, Sweden

Abstract

A constrained, two step optimization procedure based on $\mathcal{H}_\infty$ loop shaping is suggested for highly unstable plants with large parametric uncertainties. With the proposed controller synthesis, optimality is inherited from the $\mathcal{H}_\infty$ design, and robustness to uncertainties is guaranteed by use of Horowitz bounds. This implies that specifications can be made for the worst case of the sensitivity, the complementary sensitivity, and the controller sensitivity functions. The method is applied to a Tokamak fusion reactor for two different types of sensors, and in this example, optimization of one plant design parameter and one controller tuning parameter will illustrate the procedure. The results are validated by theory for performance limitations of unstable plants, as well as with a manual search over the two dimensional design and tuning parameter space.

Keywords: $\mathcal{H}_\infty$ control, Horowitz bounds, robustness, uncertainty, Tokamak, fusion, plasma

1 Introduction

Stabilization of unstable, uncertain plants can be achieved with the Quantitative Feedback Theory (QFT) by Horowitz [4], in case explicit uncertainties have been formulated for the system. The QFT can, e.g., be used to ensure that specified bounds on closed loop transfer functions are fulfilled in spite of the uncertainties. The basis for this method is a translation of the bounds on these transfer functions to so called Horowitz bounds implying restrictions on the nominal open loop. For this purpose the MATLAB toolbox QSYN [2, 8] is used. However theoretically, to achieve robust performance with QFT, infinitely many tuning parameters may be required.

In the proposed method QFT is only used as an analysis tool whereas $\mathcal{H}_\infty$ techniques are applied in the controller design implying that the tuning parameters will take the form of weight functions. Instead of manually searching for these, a constrained optimization is suggested for the tuning parameters with respect to the low frequency gain of the controller. The $\mathcal{H}_\infty$ optimization consists of two steps; an outer loop for tuning the weight function and an inner loop for the standard $\mathcal{H}_\infty$ optimization, here using the loop shaping strategy by McFarlane and Glover [9].

The theory is applied to the so called Advanced Tokamak fusion reactor, where the plasma pressure is well above the stability limit without feedback, and where equilibrium parameters can exhibit large variations. Due to the complexity of the Tokamak it is vital to keep the number of tuning parameters at a minimum, which is also the case for many other systems. An investigation of what can be achieved in terms of robust performance is carried through for the Tokamak, using two different sensor types resulting in plant transfer functions of different complexity. The results are validated with theory for performance limitations of unstable plants, as well as with a manual search over the two dimensional design and tuning parameter space.

2 Horowitz bounds

One representation of plant uncertainty is the independent parametric uncertainty. The uncertainties in the system parameters are then completely independent of one another, which leads to a great number of, or infinitely many, possible plant transfer functions. A plant having parametric uncertainty can be defined as

$$G(s) \in \{G(s,\theta)\},$$

where $\theta \in \mathrm{Q} \subset \mathbb{R}^p$ is a vector of uncertain parameters. The set of (infinitely many) transfer functions obtained by the uncertainty representation is approximated with $\{G_i(s)\}, i = 1...N$. For each frequency, $\omega_k \in \Omega$, the set $\{G_i(j\omega_k)\}$ in the complex plane is called a *template* [4]. The template should enclose all possible frequency responses of the plant at the frequency ω_k.

To be able to separate acceptable controllers from unacceptable ones, QFT can be used. This approach requires that the plant uncertainty is represented by a set of templates. Furthermore, QFT requires that the design specifications are in the form of bounds on the mag-

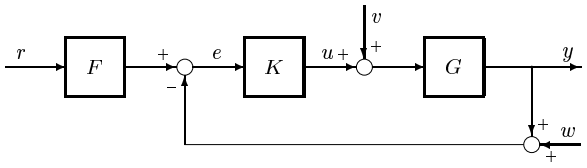

Figure 1: Closed loop system with plant G and controller K.

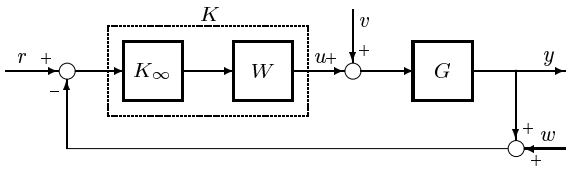

Figure 2: Closed loop system with $\mathcal{H}_\infty$ controller.

nitudes of some frequency response functions. The frequency response specifications result in constraints on the nominal open loop, $L_{nom}(j\omega) = G_{nom}(j\omega)K(j\omega)$. The constraints are called *Horowitz bounds* and reflect the interaction between the size of the plant uncertainty and the tightness of the closed loop specifications. The QFT eventually leads to a design which satisfies the specifications for all plant variations.

With the system as in Figure 1, we define

$$S_i(s) = \frac{1}{1 + G_i(s)K(s)}, \qquad i = 1, 2, ...N,$$

where G_i is the uncertain plant. Consider the design criterion $\|S_i\|_\infty \leq c_S \ \forall i$, then the following must hold:

$$M_S \equiv \max_i \left| \frac{1}{1 + G_i(j\omega_k)K(j\omega_k)} \right| \leq c_S \ \ \forall k. \qquad (1)$$

Thus, the controller will have to be chosen such that (1) is fulfilled for the complex number $K(j\omega_k)$. Clearly, for each G_i there is a domain in the complex plane of $K(j\omega_k)$ values which results in that (1) does not hold. The union of all such domains gives a domain, or possibly several domains, that contains the unacceptable values of $K(j\omega_k)$. The boundary of the domain(s) is called the Horowitz bound for $K(j\omega_k)$ with respect to the specification on the sensitivity function. Multiplying with the nominal plant yields the Horowitz bound for the nominal open loop $L_{nom} = G_{nom}K$. Bounds with respect to specifications on other closed loop transfer functions may be derived in an analogous way, e.g., for the complementary sensitivity function $M_T \leq c_T$, and for the controller sensitivity function $M_{KS} \leq c_{KS}$. From the plant templates and the specifications, the Horowitz bounds can be computed with QSYN [2], and placed in a Nichols chart together with the nominal open loop. The objective is then to loop shape the nominal open loop such that it, at each frequency ω_k, lies outside the bounds for that frequency, and such that appropriate low frequency and high frequency properties are achieved.

3 $\mathcal{H}_\infty$ controller

The $\mathcal{H}_\infty$ controller is derived in accordance with the description by McFarlane and Glover [9]. The plant $G(s)$ is shaped with a weight function $W(s)$ to give an open loop shape such that some nominal performance specifications are met. For the shaped system $\tilde{G}(s) = G(s)W(s)$, an optimal $\mathcal{H}_\infty$ controller $K_\infty(s)$, can be constructed by solving a set of riccati equations. The final feedback controller $K(s)$ for the plant $G(s)$ (see Figure 2) is then $K(s) = W(s)K_\infty(s)$. For a given weight function $W(s)$, the controller derived in this way will, in some sense, have optimal robustness (stability margins). Combined with the QFT this means that the system keeps up stability and bandwidth in the face of uncertainties caused by unmodeled high frequency dynamics, low frequency parameter variations and different disturbances.

4 Limitations

When trying to control plants with right half plane (RHP) poles, the primary objective will be to stabilize the plant. The stabilization will impose limitations on closed loop performance, and especially on $\|S\|_\infty$ and $\|T\|_\infty$. Havre and Skogestad [3] have shown how these limitations may be calculated in a simple way and the procedure is partly described below.

Consider an unstable plant $G(s)$, and the factorization

$$\begin{aligned} G(s) &= \mathcal{B}_z(s)\mathcal{B}_p^{-1}(s)G_{ms}(s), \\ \mathcal{B}_z(s) &= \prod_{j=1}^{N_z} \frac{s - z_j}{s + \bar{z_j}}, \ \ \mathcal{B}_p(s) = \prod_{i=1}^{N_p} \frac{s - p_i}{s + \bar{p_i}}, \end{aligned} \qquad (2)$$

where N_p is the number of RHP poles $p_i \in \mathbb{C}$, N_z is the number of RHP zeros $z_j \in \mathbb{C}$ in G. $\bar{p_i}$, $\bar{z_j}$ denotes the complex conjugates of p_i, z_j, and $(\cdot)_{ms}$ denotes the stable and minimum phase version of the associated transfer function. Assume $N_z \geq 0$, $N_p \geq 1$ and that TV is internally stable, where T is the complementary sensitivity function, and V is an arbitrary weight function. Then the following lower bound on $\|TV\|_\infty$ applies:

$$\|TV\|_\infty \geq \max_{p_i} |\mathcal{B}_z^{-1}(p_i)||V_{ms}(p_i)|. \qquad (3)$$

Now consider the choice $V = G^{-1}$ and assume there are no RHP zeros and one RHP pole p. It is seen that $\|TV\|_\infty = \|KS\|_\infty$ for this choice of V and by using (3), a lower bound of the $\mathcal{H}_\infty$ norm of the controller sensitivity function KS is obtained as

$$\|KS\|_\infty \geq |G_{ms}^{-1}(p)|. \qquad (4)$$

Table 1: Plant transfer functions for two different sensors.

eq.	$B_{\theta 1}$		$B_{\theta 2}$	
	$P_1(s)$	$P_2(s)$	$P_1(s)$	$P_2(s)$
1	$\frac{2.38s+1}{0.714s^2-0.263s-0.288}$	$\frac{0.373s^2+0.132s-0.114}{0.714s^2-0.263s-0.288}$	$\frac{5.73s^2+17.1s+3.44}{1.56s^3+4.05s^2-3.36s-1}$	1
2	$\frac{0.449s+1}{0.0870s^2+0.0533s-0.449}$	$\frac{0.0349s^2+0.116s-0.219}{0.0870s^2+0.0533s-0.449}$	$\frac{1.06s^2+2.53s+2.23}{0.213s^3+0.122s^2-0.576s-1}$	1
3	$\frac{0.441s+1}{0.0596s^2-0.0226s-0.525}$	$\frac{0.0141s^2+0.0903s-0.241}{0.0596s^2-0.0226s-0.525}$	$\frac{0.193s^2+1.31s+1.91}{0.0259s^3+0.109s^2-0.287s-1}$	1
4	$\frac{0.454s+1}{0.0376s^2-0.158s-0.683}$	$\frac{0.00814s^2+0.0298s-0.395}{0.0376s^2-0.158s-0.683}$	$\frac{0.125s^2+0.913s+1.47}{0.0104s^3+0.00896s^2-0.403s-1}$	1

This will in fact hold for any linear controller in order to stabilize the plant. Note that the lower bound on $\|KS\|_\infty$ is independent of the controller, since the chosen weight V in (3), does not depend on the controller. By choosing the weight differently and by using an analogous theorem for the sensitivity function, suggested in [3], lower bounds on other closed loop transfer functions may also be obtained.

5 Controller design for an advanced Tokamak reactor

5.1 Electromagnetical background

The most successful device for confining thermonuclear plasmas is the Tokamak, which relies on confinement by magnetic fields. The large scale dynamics of the Tokamak is well described by magnetohydrodynamics (MHD). Although Tokamaks can be operated in such a way as to be stable within the MHD model, large improvements in terms of performance are made possible by exceeding such operational limits. In such scenarii one has to rely on external feedback to stabilize the plasma.

By using a plasma cross section that is elongated in the vertical direction, the limits of plasma pressure can be significantly increased at the expense of introducing *one* single instability corresponding to a rigid shift of the plasma in the vertical direction. Because of its simple mode structure (toroidal mode number is $n = 0$), this instability is relatively simple to control and this was accomplished in the eighties, see [5]. The control relies on the existence of a nearby electrically conducting wall. The wall has to be placed sufficiently near the plasma so that all MHD modes would be stable if the wall were super conducting. However, magnetic perturbations penetrate a finitely conducting wall on the time scale of resistive diffusion (which can be expressed as L_w/R_w where L_w is the inductance and R_w the resistance of the eddy current pattern on the wall), see Figure 3. This time scale is typically of the order of several ms, whereas MHD instabilities that are not stabilized by a conducting wall typically occur on μs time scales. The wall slows the growth of MHD instabilities and the feedback system only needs to respond on a much slower time scale. The feedback system need to generate currents in active coils that oppose the magnetic fields produced by the MHD instability. A good description of a control system for vertical control can be found in [10]. For the so called advanced Tokamak, it is desirable to increase the pressure even further and this leads to instability also for modes with toroidal mode number $n = 1$. The structure of $n = 1$ modes is more complicated and therefore the geometrical design of sensor and feedback coils becomes a more delicate issue. In [7] it was shown that by using a sensor of "radial" magnetic field perturbations (normal to the wall), control should be possible if the sensor coil is close to the plasma. It has now been realized that sensors for the "poloidal" magnetic field B_θ (tangential to the wall), are more effective and allows better control, even with the sensors rather far away from the plasma, see [1, 6].

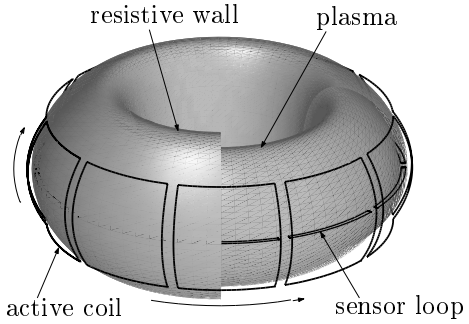

Figure 3: Plasma

5.2 Plant model and specifications

The Tokamak is modeled by finite element method techniques (using an MHD stability code) which can be used to compute open loop transfer functions of an unstable plasma, see [7]. The transfer functions take the following form:

$$G(s) = \frac{P_1(s)}{1 + s\tau_f P_2(s)}. \tag{5}$$

$G(s)$ gives the ratio of flux measured by the sensor coil to the current in the feedback coil, and is typically given as third, or fourth, order Padé approximations. With this transfer function, we design a controller subject to realistic constraints on amplifier response time etc. The early theoretical work, see [7], assumed an ideal current source with zero response time $\tau_f = L_f/R_f$. From the control viewpoint, the immediate goal of the plant design is to maximize τ_f, such that reasonable stability margins are obtained for moderate control signals. This means that the problem takes quite an interesting form, since by designing the control system, we have the opportunity to affect the construction of the Tokamak plant!

From the linearization of the plant model, four significantly different equilibria have been chosen for two sensors of different complexity, see Table 1. The sensors are denoted $B_{\theta 1}$ and $B_{\theta 2}$, and results in the two systems G_{B1} and G_{B2}. The Bode plots of the linearized systems are shown in Figure 4.

With its large uncertainties and with the large magnitude of the RHP pole, stabilizing the Tokamak at the same time as achieving robust performance will be a difficult task. The trade off between properties in different frequency regions, such as low frequency performance and mid/high frequency robustness is evident. Due to economic reasons, the most important specification will be to keep the control signals low (M_{KS}), whereas the specifications on the stability margins (M_S and M_T) can be somewhat looser. The specifications considered are:

$$M_S \leq 2.5, \quad M_T \leq 2.5, \quad M_{KS} \leq 10. \tag{6}$$

5.3 Controller design

Considering the fourth equilibria and using the theory in Section 4, the minimum control activity required for stabilizing the plants were computed for $\tau_f = 3$, 2, 1, 0.5 and 0.25, see Figure 5.

From this entirely theoretical result, it is seen that, in order to get control signals in the neighborhood of the specification (6), $\tau_f \approx 1$ will have to be chosen for G_{B2}. It is important to remember that this is only with respect to the fourth equilibria, and that when considering the entire uncertainty interval, $\|KS\|_\infty = 10$ might not at all be enough to stabilize G_{B2} when $\tau_f \approx 1$. The result gives merely an idea of the region of interest for τ_f.

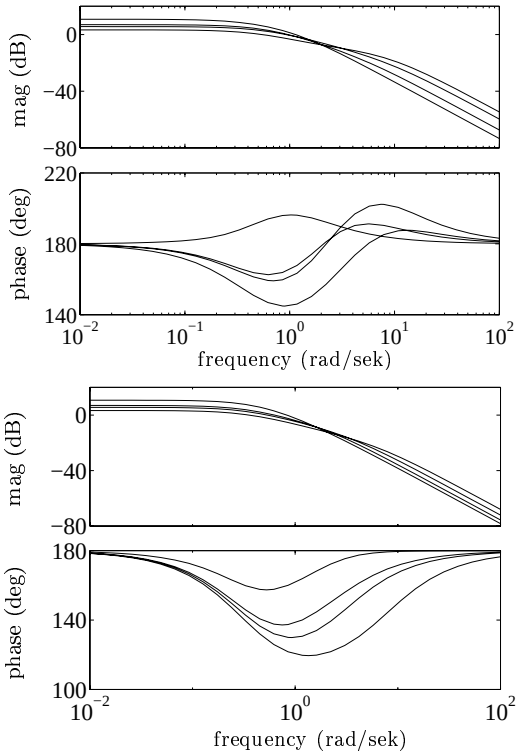

Figure 4: Bode plot of the four equilibria in Table 1 for G_{B1} (top) and G_{B2}(bottom).

Assigning a fixed value for τ_f will imply that also the model is fix, see (5), and the linearized model can then be interpreted as that the uncertainty in the model only depends on the four different versions of the transfer functions P_1 and P_2. By use of (5) and Table 1, the transfer functions takes the form

$$G(s) = \frac{a_2 s^2 + a_1 s + a_0}{b_4 s^4 + b_3 s^3 + b_2 s^2 + b_1 s + b_0}, \tag{7}$$

where $a_2 = b_4 = 0$ for G_{B1}. After choosing a nominal plant, the Horowitz bounds for $M_S \leq c_S$, $M_T \leq c_T$, and $M_{KS} \leq c_{KS}$ may be computed using the technique described in Section 2. With these bounds and the controller tuning parameters ρ, as inputs, the following two step $\mathcal{H}_\infty$ optimization is suggested:

$$\max_{\rho} \tau_f, \quad s.t. \quad \begin{cases} M_S & \leq & 2.5 \\ M_T & \leq & 2.5, \\ M_{KS} & \leq & 10. \end{cases} \tag{8}$$

However, since τ_f is a system parameter it is not suitable as a performance index. A more convenient approach is to maximize the low frequency gain of the controller, which is closely related to load disturbance attenuation, for a given τ_f and then increase τ_f (until the constraints no longer can be met). This will result in a number of designs, where the design with the maximum τ_f is sought for. By using the result in Figure 5, we already know the region of interest for τ_f and hence, the maximum can be found rather quickly.

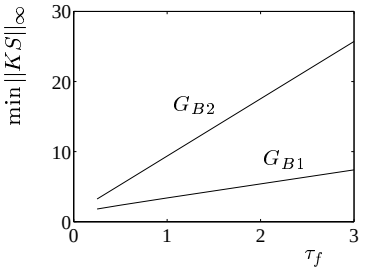

Figure 5: Minimum control activity, for the fourth equilibra, as a function of τ_f.

For a given τ_f, the Horowitz bounds were computed with respect to the specifications (6), using 16 equidistant points for each of the uncertain parameters in (7). An example of the Horowitz bounds for the sensitivity function with respect to G_{B1} (for a fixed τ_f) is shown in a Nichols plot in Figure 6, with a 360^o phase shift of the nominal system. Then, choosing W as a frequency independent weight, the constrained $\mathcal{H}_\infty$ optimization was performed in two steps with the Horowitz bounds as constraints. An outer loop for tuning the weight function and an inner loop for the standard $\mathcal{H}_\infty$ optimization (choosing slightly suboptimal solutions).

The resulting controllers were of order 4, and the optimization results can be seen in Table 2. Also shown in Table 2 are the maximum of the $\mathcal{H}_\infty$ norms of S, T, and KS over the uncertainty interval when the proposed τ_f and W is used. From the table we find that the specifications are fulfilled, as expected. Recalling the linearization and the four equilibria in Table 1, it is seen that the average of the low frequency limit of $P_2(s)$ for G_{B1} is 0.48, whereas it equals 1 for G_{B2}. Normalizing τ_f with this average low frequency limit will give a fair comparison between the two sensors, and results in a quotient $(\tau_{f,B1}/\tau_{f,B2})_{normalized} = 2.67$ which means that the $B_{\theta 1}$ sensor is to prefer.

We also choose to study the step responses from input disturbance $v(t)$ to output $y(t)$, from reference $r(t)$ to

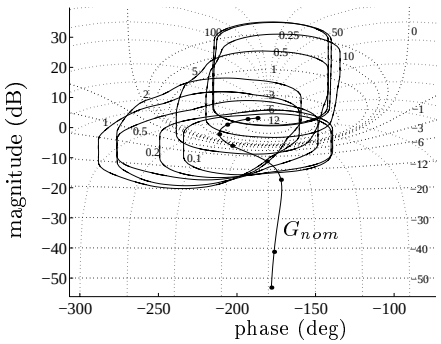

Figure 6: Nominal plant with 360^o phase shift and Horowitz sensitivity bounds for G_{B1}.

Table 2: Optimization results and the resulting M_S, M_T, and M_{KS} for both plants.

Plant	W	τ_f	M_S	M_T	M_{KS}
G_{B1}	2.5	2.5	1.7	2.5	10
G_{B2}	2.35	0.45	2.0	2.5	10

control signal $u(t)$, and from reference to output, for both plants with the proposed values of τ_f and W, see Figure 7. It is clear that by choosing the $B_{\theta 2}$ sensor we will obtain faster rise times and settling times, though at the cost of a considerably lower value of τ_f.

Having these results, the design is complete. Though, for further reference, the relations between τ_f, $\|T\|_\infty$, $\|S\|_\infty$, and $\|KS\|_\infty$ are studied more closely. For a fixed value of τ_f, $\|S\|_\infty = f(\|KS\|_\infty)$ and $\|T\|_\infty = f(\|KS\|_\infty)$ were manually computed, and are shown in Figures 8 and 9 for the fourth equilibria of the two plants. Studying these, we clearly see the trade off between stability margins and control activity. That is, for a given value of τ_f and a restricted control activity (fixed $\|KS\|_\infty$), considerably higher values of the stability margins $\|S\|_\infty$ and $\|T\|_\infty$ are obtained for G_{B2}, compared to G_{B1}. Besides, in Figure 8 we also note the asymptotic behaviour which confirms the theoretical result in Figure 5.

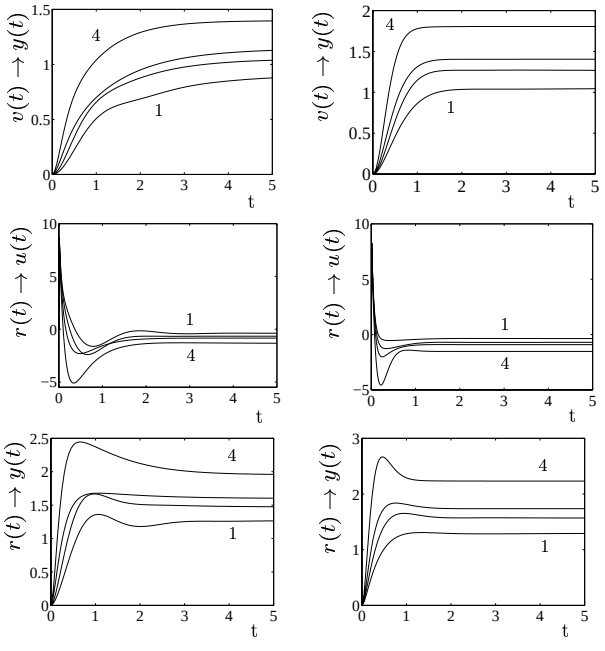

Figure 7: Step responses for the fourth equilibria of G_{B1} (left), $\tau_f = 2.5$, $W = 2.5$, and G_{B2} (right), $\tau_f = 0.45$, $W = 2.35$.

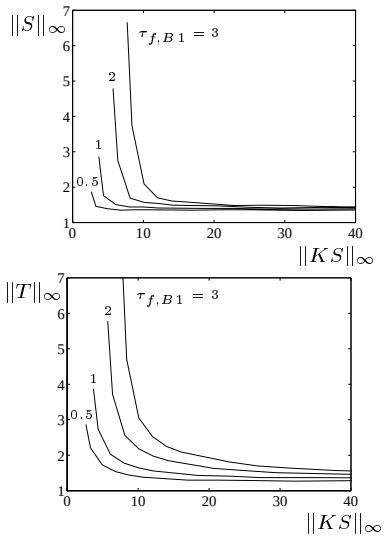

Figure 8: $\|S\|_\infty$ and $\|T\|_\infty$ as a function of $\|KS\|_\infty$ for the fourth equilibria of G_{B1}.

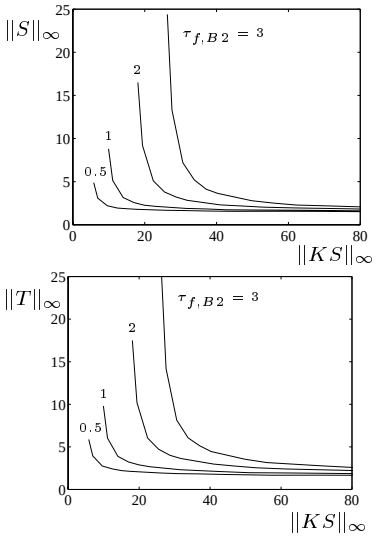

Figure 9: $\|S\|_\infty$ and $\|T\|_\infty$ as a function of $\|KS\|_\infty$ for the fourth equilibria of G_{B2}.

6 Conclusions

A constrained, two step optimization procedure based on $\mathcal{H}_\infty$ loop shaping for highly unstable plants with large parametric uncertainties has been suggested. Robustness to the uncertainties are guaranteed by use of Horowitz bounds for the sensitivity function S, the complementary sensitivity function T, and the controller sensitivity function KS.

The method has been applied to a Tokamak fusion reactor for two different types of sensors, including optimization of one plant design parameter and one controller tuning parameter. This means that when the design parameter τ_f is assigned there will only be one tuning parameter for the operator. The results show that all specifications have been achieved for both sensors. In addition, it has been shown that by choosing one of the suggested sensors, rise times and settling times can be reduced, though at the cost of a considerably lower value of the design parameter τ_f. Finally, a validation of the $\mathcal{H}_\infty$ optimization has been carried through by using theory for performance limitations of unstable plants, as well as using a manual search over the two dimensional (design and tuning) parameter space.

The suggested design procedure, based on the inherent optimality and robustness properties of the $\mathcal{H}_\infty$ loop shaping, is simpler compared to ordinary QFT. The resulting controller of order 4 has a single parameter to tune the trade off between stability margins and control activity, when explicit uncertainties for the unstable plant are taken into account.

References

[1] C. M. Fransson, B. Lennartson, C. Breitholtz, Y. Q. Liu, and A. Bondeson. Feedback stabilization of non-axisymmetric resistive wall modes in tokamaks. part 2: Control analysis. *The Physics of Plasmas*, 2000. To appear.

[2] P. O. Gutman. *QSYN the toolbox for robust control systems design for use with Matlab*, 1996.

[3] K. Havre and S. Skogestad. Performance limitations for unstable SISO plants. In *Proc. Amer. Control Conference*, pages 3234–3238, Philadelphia, June 1998.

[4] I. Horowitz. *Quantitative Feedback Design Theory (QFT)*. QFT Publications, Chicago, USA, 1993.

[5] E. A. Lazarus, J. B. Lister, and G. H. Neilson. Control of the vertical instability in tokamaks. *Nuclear Fusion*, 30:111–141, 1990.

[6] Y. Q. Liu, A. Bondeson, C. M. Fransson, B. Lennartson, and C. Breitholtz. Feedback stabilization of non-axisymmetric resistive wall modes in tokamaks. part 1: Electromagnetical model. *The Physics of Plasmas*, 2000. To appear.

[7] Y. Q. Liu and A. Bondesson. Active feedback stabilization of toroidal external modes in tokamaks. *Phys. Rev. Lett.*, 84(5):907–910, 2000.

[8] MathWorks. *Matlab Optimization Toolbox, User's Guide*. Natick, MA, USA, 1996.

[9] D. McFarlane and K. Glover. A loop shaping design procedure using $\mathcal{H}_\infty$ synthesis. *IEEE Trans. Autom. Contr.*, 37(6):759–769, 1992.

[10] P. Vyas, D. Mustafa, and A. W. Morris. Vertical position control on compass-D. *Fusion Technology*, 33:97–105, 1998.